Chemical Engineering Journal 462 (2023) 142088

Contents lists available at ScienceDirect

Chemical Engineering Journal

journal homepage: www.elsevier.com/locate/cej

High-rate and -yield continuous fluidized-bed bioconversion of glucose-to-gluconic acid for enhanced metal leaching

Payam Rasoulnia *, Réka Hajdu-Rahkama, Jaakko A. Puhakka

Tampere University, Faculty of Engineering and Natural Sciences, P.O. Box 541, FI-33104 Tampere, Finland

ARTICLE INFO

Keywords:
Fluidized-bed bioreactor
Gluconobacter oxydans
Leptobacillium leptobactrum
Non-aseptic
Rare earth elements
Spent battery recycling

ABSTRACT

Continuous low-cost bulk biolixiviant production remains as one of the main challenges of heterotrophic bioleaching towards large scale application. This study aimed at developing non-aseptic *Gluconobacter oxydans*-amended fluidized-bed reactor (FBR) process for continuous production of gluconic acid for efficient leaching of rare earth elements (REEs) and base metals from spent nickel-metal-hydride (NiMH) batteries. In preliminary experiments, the FBR became contaminated and massively overgrown by air-borne fungus, *Leptobacillium leptobactrum*. In a series of batch bioassays, operational conditions were investigated to discourage the fungal activity i.e., an ecologically engineered niche for gluconic acid production. High gluconate concentration (≥100 g/l) and/or low pH (≤2.5) gave a selective preference for *G. oxydans* growth over *L. leptobactrum* and controlled the activity of possible contaminants during FBR continuous operation. The highest gluconic acid production rate of 390 g/l•d with corresponding glucose-to-gluconic acid conversion yield of 94% was obtained at hydraulic retention time (HRT) of 6.3 h and 380 g/l•d glucose loading rate. Using the FBR effluents as leaching agents, respectively, total base metals and REEs leaching yields of up to 82% and 55% were achieved within 7 days at 1% (w/v) spent battery pulp density. The obtained glucose-to-gluconic acid conversion rates and yields were one of the highest reported for any glucose biotransformation process. The REE leaching yields were higher than those reported for similar high metal-grade REE secondary sources. The high-rate glucose-to-gluconic acid bioconversion in the non-aseptic system utilizing microbial ecology based FBR operation strategy rather than aseptic chemostats indicates industrial feasibility of gluconic acid production and thus, the applicability of heterotrophic bioleaching.

1. Introduction

Rapid increase in global electric vehicles (EVs) production has resulted in substantial demand of battery raw materials including rare earth elements (REEs), Li, Ni, and Co. Today's number of EVs of approximately 7.2 million is estimated to increase to over 245 million by the year 2030 [1]. Nickel-metal-hydride (NiMH) and Li-ion batteries are two major EV battery types representing about 28% and 37% of the world's rechargeable battery market, respectively [2]. Given the limited lifetime of EV batteries, a huge quantity of spent battery materials would require new recycling technologies in near future [3]. Recycling these spent batteries is crucial not only to sustain the raw materials supply but also to overcome the environmental and supply challenges related to metal mining from natural resources [4].

Due to their high cobalt (3–5%), nickel (36–42%), and REEs (5–25%) content, spent NiMH batteries are increasingly investigated for recycling [2]. Current physico-chemical technologies for recycling spent NiMH batteries are energy intensive, complex, costly and environmentally hazardous [5]. Heterotrophic bioleaching is a potential alternative method that uses microorganisms to produce different organic acids from organic substrates such as glucose [6,7]. Heterotrophic bioleaching can be carried out using either contact or non-contact bioleaching methods. In contact bioleaching, the metal-containing solid material is directly added to the microbial culture and thus, the metal leaching and solvent production take place simultaneously in the same vessel [8]. Contrarily, in non-contact bioleaching process, the microbial leaching agent is first produced by microorganisms in absence of the metal-containing solid material and then the bio-produced leaching solution is used for metals extraction from the solid material in a separate vessel [8,9].

Metal leaching using biologically produced organic acids is advantageous over conventional methods that apply inorganic acids with high

* Corresponding author.
E-mail address: payam.rasoulnia@tuni.fi (P. Rasoulnia).

https://doi.org/10.1016/j.cej.2023.142088
Received 8 December 2022; Received in revised form 27 January 2023; Accepted 20 February 2023
Available online 28 February 2023

temperatures as it is more environmentally friendly, requires less energy, and enhances the overall metal dissolution due to contribution of complexation leaching mechanism in addition to protonation [10,11]. So far, several batch studies with heterotrophic microorganisms such as *Gluconobacter oxydans*, *Aspergillus niger* and *Komagataeibacter xylinus* have been reported for REE leaching from various end-of-life products [6,12–15]. Continuous process bioleaching studies are scarce albeit offering several advantages over batch processes including [16]: (1) less time needed for inoculum preparation, and filling in, emptying, cleaning or sterilizing the plant, (2) stable product quality due to constant process conditions and feed composition, (3) possibility for continuous downstream processes together with reduced production costs, and (4) low investment costs for large-scale production due to higher volumetric productivity.

G. oxydans is a non-pathogenic gluconic acid producing bacterium with high REE leaching capability [15]. So far, several non-bioleaching related studies have focused on production of gluconic acid with different microorganisms [16–24]. However, these studies mostly lack concomitant high-rate and -yield gluconic acid production and have been conducted under fully aseptic and non-acidic pH conditions (4.3–6.5) which is not optimal for bioleaching purposes. High-rate and -yield continuous bioproduction of low-cost leaching agent under non-aseptic conditions remains one of the main bottlenecks for further development of heterotrophic bioleaching processes at large-scale applications. Therefore, this study aimed at developing a strategy for high-rate and -yield continuous production of gluconic acid using a non-aseptic *Gluconobacter oxydans*-amended fluidized-bed reactor (FBR). In a series of batch assays, process conditions that minimize contamination of the non-aseptic operation and enable high-rate and -yield glucose-to-gluconic acid bioconversion were determined. Finally, the FBR effluent solutions were used for non-contact bioleaching of base metals and REEs from the spent NiMH battery powder at different pulp densities.

2. Materials and methods

2.1. Microorganism and growth conditions

Gluconobacter oxydans (DSM 3503) obtained from German Collection of Microorganisms and Cell Cultures (DSMZ) was used. A glucose-yeast extract (GY) medium consisting of (g/l) glucose (100), yeast extract (YE) (10), agar (15), and $CaCO_3$ (20) was used to maintain *G. oxydans* stock culture. An autoclaved medium containing (g/l) $CaCl_2{\cdot}2H_2O$ (0.044), $(NH_4)_2SO_4$ (0.5), NaCl (0.2), KCl (0.2), $MgSO_4$ (0.1) with varying concentrations of YE and glucose (G) at a mass YE/G ratio of 0.08 (YE medium) was used for all the experiments [13]. Some modifications of this medium were applied as an experimental variable. The incubation temperature was 27 ± 1 ∘C.

2.2. Isolation of the fungal contaminant and identification by DNA extraction and sequencing

Samples for isolation of the contaminant fungus were taken from the FBR and the aeration unit (AU). The fungal contaminant was isolated by repetitive transferring of the samples to GY agar culture plates. The GY agar medium composition was as described in section 2.1. The agar media were inoculated with 1 ml FBR samples. The fungal colonies were whitish and easily separable from those of *G. oxydans*. From these plates, the whitish fungal colonies were transferred to new GY agar plates and followed by incubation and several retransfers and cultivations. After this phase, the fungal isolates were grown in a YE liquid medium and used for identification.

The contaminant isolated from the FBR as well as the direct FBR sample were used for identification by fungal Internal Transcribed Spacer (ITS) amplicon sequencing. Prior to the sequencing, 2 ml of the contaminated liquid samples were collected and centrifuged at 2800 relative centrifugal field(rcf) and 4 °C for 15 min. The cell pellets were then used for DNA extraction using DNeasy PowerSoil Kit (Qiagen) [25]. The extracted DNA samples were sent for Amplicon Metagenomics Sequencing (WBI) Species Fungal Sequencing to Novogene UK. The amplified region was ITS2 with a fragment length of 380 bp [26]. The forward and reverse primers used were ITS3-2024F (GCATCGATGAAGAACGCAGC) and ITS4-2409R (TCCTCCGCTTATTGATATGC), respectively. Basic bioinformatics analysis (amplicon metagenomics sequencing) was prepared by Novogene UK.

2.3. Fungal growth under extreme conditions

The growth of the contaminant fungus was examined under different growth extremes including low initial pH and high gluconate concentration in the presence or absence of glucose. Different initial pH values including 2.3, 2.5, and 2.7 were used in a YE medium containing 10 g/l glucose. The different potassium gluconate concentrations of 10, 25, 50, 100, 125, and 150 (g/l) were used in a YE medium with an initial pH of 2.7, in presence and absence of 10 g/l glucose. The glucose utilization rates by the contaminant fungus and *G. oxydans* were determined using a YE medium containing 10 g/l glucose. The experiments were carried out in 250 ml shake flasks containing 100 ml of the media inoculated by 5–7 days old agar culture plates of the fungus or *G. oxydans*. The shake flasks were rotated at 150 rpm for 6 days and the growth characteristics including pH, optical density (OD_{600}), and gluconate concentration were monitored regularly. The initial pH in the media were adjusted using 65% nitric acid.

2.4. Bioreactor design and operation

The continuous production of gluconic acid was investigated in a *G. oxydans*-amended FBR coupled with an AU for aeration (Fig. 2). Both the FBR and AU had a diameter of 4.5 cm and a working volume of 170 ml. The reactor parts were autoclaved prior to adding the carrier material. Granular activated carbon (AC) (Filtrasorb 200, Calgon Carbon Corporation, USA) with effective and mesh sizes of 0.55–0.75 mm and 12x40 was used as the carrier material for *G. oxydans* biofilm formation. The fluidized-bed volume was 91 ml. Prior to use in the FBR, the AC was washed with acidic Milli-Q water to a pH of 2 and heated overnight at 105 °C. The volume of AC used in the FBR was 70 ml. To retain the carrier material in the reactor and also to disperse the liquid flow, one big glass bead with a diameter of 25 mm was used at the bottom of the FBR. The FBR was kept at room temperature (27 ± 1 ∘C) during the operation. To minimize the entrance of air bubbles into the FBR, aeration was supplied from the bottom of the AU. The inlet air passed through a 0.2 μm filter (FG, F1AB79505) prior to entering the AU. The aeration rate was controlled at 0.15 ± 0.02 NL/min using a manual flow meter (Kytola Instruments, Finland). The recirculation flow rate was set at 340 ± 20 ml/min to obtain 30% fluidization of the AC bed using a peristaltic pump (Master flex, Cole-Parmer, USA). The recycle flow rate was approximately 1300 times higher than that of the feed flow rate resulting in a completely mixed bioreactor system.

In the start-up phase of continuous FBR operation (day 0 to 5), a YE medium containing 10 g/l glucose, ~100 g/l potassium gluconate, and 10% (v/v) *G. oxydans* inoculum was used as the start solution. During the start-up phase, the feed composition and flow rate were changed as demonstrated by A-D1 in Fig. 1. From day 5 onwards, the feeding flow rate and thus, the hydraulic retention time (HRT) were held constant at 0.24 ml/min and 6.3 h, respectively. During the 41 days (day 5 to day 46) continuous operation of the FBR, different glucose loading rates were evaluated by stepwise increase of the feed glucose concentration from 50 to 75 and 100 g/l. Daily samples were taken from the effluent for pH, glucose, and organic acid analyses. The antifoaming agent (antifoam 204, sigma Aldrich) concentration in the feed was kept at 0.01–0.02% to control foam formation.

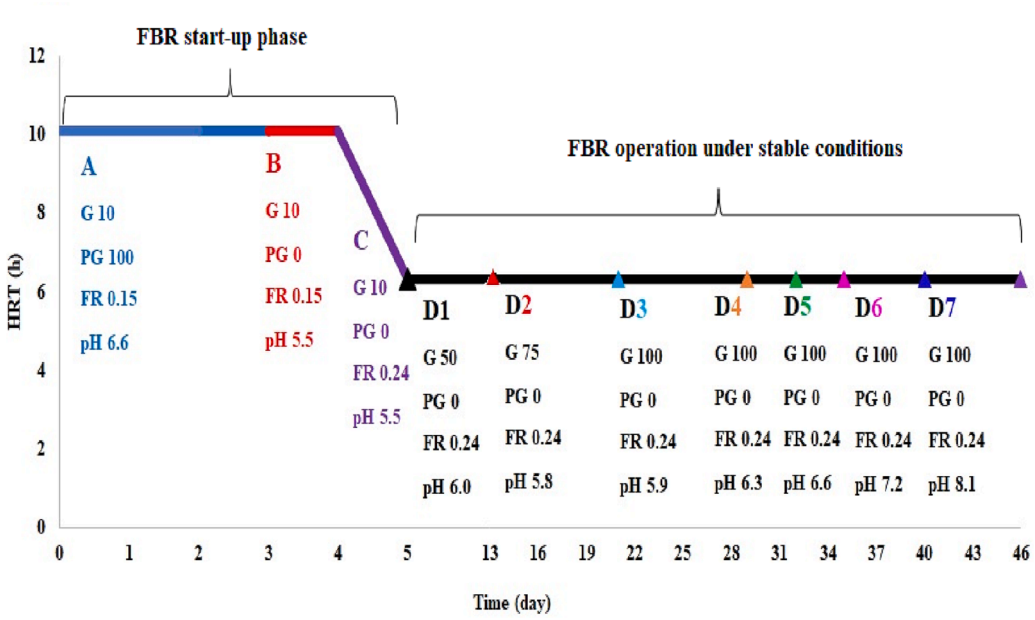

Fig. 1. *G. oxydans*-amended FBR in-feed conditions; G represents glucose g/l, PG represents potassium gluconate g/l, FR represents feed flow rate ml/min, and pH represent feed acidity. A, B, C, and D1 to D7 show the changes of parameters during different experimental steps.

2.5. Spent NiMH battery composition and leaching experiments

The spent NiMH battery was supplied by the battery recycling company of AkkuSer Oy in Finland. The battery powder had a particle size of less than 630 μm and contained a variety of different REEs and base metals (Table 1). The leaching of the spent NiMH battery was conducted in 50 ml metal-free polypropylene tubes using 20 ml of the bio-produced gluconic acid solution obtained from the FBR effluent under the different glucose loading rates of 190, 285, and 380 g/l•d. The tested spent battery pulp densities in the leaching experiments were 1, 3, 5, 7, and 10% (w/v). The leaching rotation speed, temperature, and duration were respectively, 150 rpm, 27 ± 1 °C, and 7 days. The REEs and base metals leaching yields at different pulp densities were evaluated by taking samples on days 1 and 7.

2.6. Biomass estimation

The *G. oxydans* biomass from both the FBR carrier material and the liquid phase was estimated by bacterial staining with 4′, 6-diamidino-2-phenylindole (DAPI) and using epifluorescence microscopy. For cell detachment from the carrier material, 1 g of AC was washed with 10 ml washing solution containing (g/l) 0.1 peptone, 0.38 ethylene glycol tetra acetic acid (EGTA), 0.000335 Zwittergent 3–12 and 3.728 KCl. The samples including the washing solution were sonicated (40% amplitude) 5 times for 1 min intervals and 30 s breaks in between [27]. The pH of the washing solution was adjusted to 2.5 using 2 M HCl, and the solution was sterilized by filtering through 0.2 μm filters (CHROMAFIL® Xtra PET-20/25, Germany). The collected samples from the AC material and the liquid medium were diluted 100 and 50 times, respectively, prior to DAPI staining. Autoclaved Milli-Q water with a pH of 2.5 was used for sample dilution. The cells of DAPI stained samples were calculated by using the Most Probable Number technique [28].

2.7. Analytical methods

The gluconic acid and 5-ketogluconic acid concentrations were determined by high performance liquid chromatography (HPLC) using a Shimadzu (SIL-40C series, Japan) device equipped with an Aminex HPX-87H column (300 × 7.8 mm) and a diode array detector at 210 nm. For the gluconic acid analysis, the mobile phase was 20 mM sulfuric acid with a flow rate of 0.5 ml/min. The sample injection volume was 2 μl, the column temperature was 50 °C and the stop time was 30 min. The glucose concentration was analyzed using a Shimadzu HPLC (SIL-20 series, Japan) equipped with a Shodex column (HILICpak, VG-50 4E) and a refractive index detector under the following conditions: sample injection volume 5 μl, mobile phase flow rate 0.2 ml/min, the column temperature 40 °C and the stop time 40 min. For the glucose analysis, the samples were mixed with acetonitrile at a 30–70% ratio (v/v) and the mobile phase was a 70–30% (v/v) mixture of acetonitrile and 0.5% NH_3 (aq). Throughout the experiments, the optical density (OD_{600}) and pH of the samples were measured using an Ultrospec 500 pro spectrophotometer (Amersham Biosciences, England) and a pH meter (pH 3110, WTW, Germany) with a Hamilton Slimtrode electrode. Milli-Q water was used as blank for measuring OD_{600}. The dissolved oxygen (DO) was online monitored using a digital oxygen sensor (Oxymax, Endress Hauser, Germany). The metal concentrations in the leaching solutions were measured using inductively coupled plasma mass spectrometry (iCAP RQ ICP-MS, Thermo Scientific, USA). The measurements were conducted in kinetic energy discrimination mode using He as collision gas and Ar as the carrier gas. The samples were 1000-fold diluted using 2% ultrapure HNO_3. The samples were filtered through 0.2 μm disposable syringe filters (CHROMAFIL® Xtra PET-20/25, Germany) for both ICP-MS and HPLC analyses.

3. Results

3.1. Contamination of G. oxydans-amended FBR and contaminant identification

In the two initial attempts to operate the *G. oxydans*-amended FBR, a semi-batch mode (~7 days) was used to form *G. oxydans* biofilm on the AC carrier material followed by switching to continuous mode. A YE medium with 50 g/l glucose was fed semi-continuously or continuously at 0.15 ml/min. Under the utilized conditions and within one-week, fungal contamination occurred in the FBR as visualized in Fig. S1 and confirmed by the molecular analyses. Due to the fungal contamination, the *G. oxydans*-amended FBR operation for gluconic acid production failed in both cases. In the ITS DNA sequencing technique and

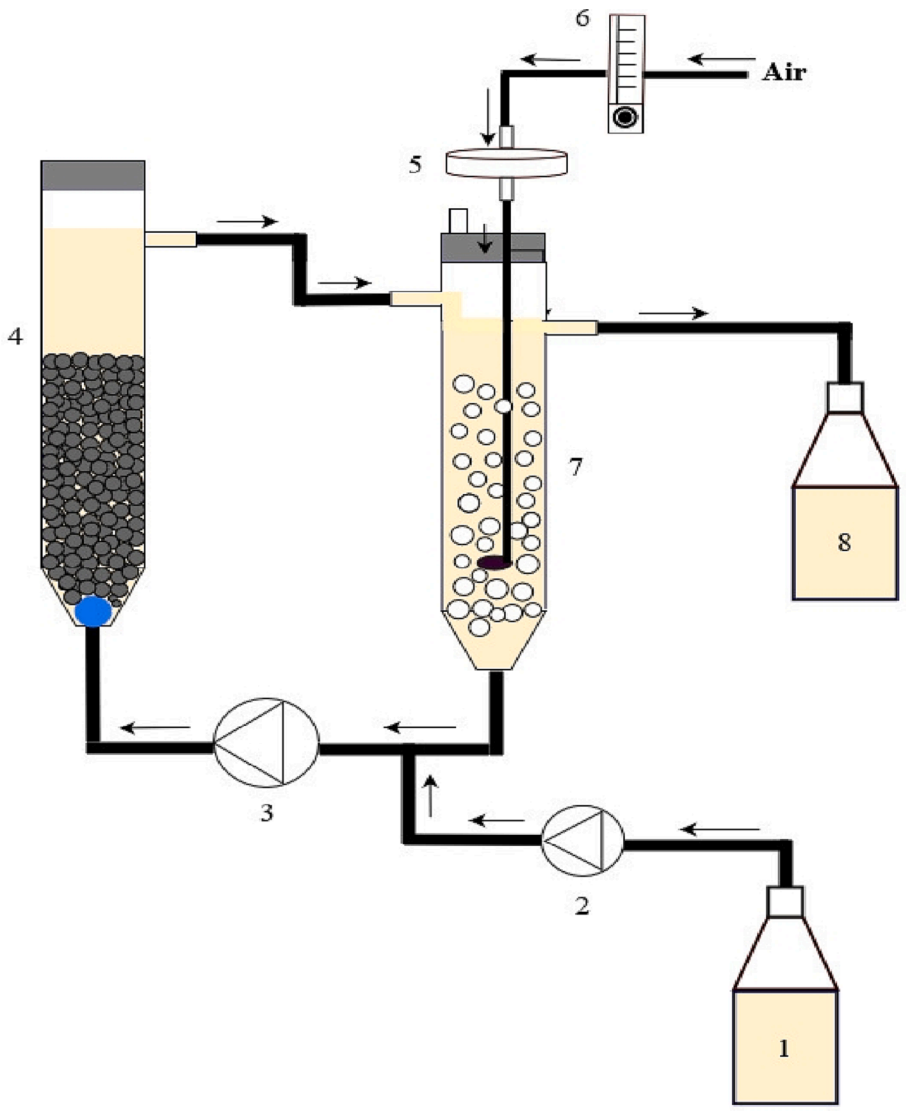

Fig. 2. Schematic diagram of the fluidized bed bioreactor system: (1) feed tank, (2) feed pump, (3) recirculation pump, (4) fluidized bed bioreactor, (5) air filter, (6) airflow meter, (7) aeration unit (AU), (8) effluent tank.

Table 1
Spent NiMH battery powder composition.

Element	Spent NiMH battery content (g/kg)
Ni	435.21
Co	90.84
Mn	22.00
Cu	12.31
Zn	8.78
Fe	4.86
La	102.27
Ce	59.51
Nd	29.56
Pr	9.88
Sm	2.96
Y	1.54
Yb	0.48
Gd	0.37
Er	0.24
Tb	0.02
Dy	0.01

Operational Taxonomic Units (OTU) analysis, the relative abundance of Ascomycota phylum in the microbial community in the FBR carrier material was over 97% (Fig. 3a). The contaminant fungus was identified as *Leptobacillium leptobactrum* with >86% relative abundance (Fig. 3b). Another species detected in the FBR sample was *Aureobasidium pullulans* with >9% relative abundance, whereas in the isolated samples (FUNG1. LIQ and FUNG2.LIQ), >99% was *L. leptobactrum*.

3.2. Extreme conditions limiting *Leptobacillium leptobactrum* growth

In order to avoid the *G. oxydans*-amended FBR contamination, a series of batch assays were carried out to determine process conditions that would favor gluconic acid production by *G. oxydans* and simultaneously minimize the fungal contamination. Based on the results, an operational FBR start-up strategy was developed to avoid contamination and obtain high-rate and high-yield glucose-to-gluconic acid bioconversion. The effects of low initial pH and high gluconate concentrations on the growth of the FBR contaminant *L. leptobactrum* were investigated and the results were as shown in Fig. 4, S2, S3, and S4.

The low initial pH values of 2.7, 2.5, and 2.3 were used. At initial pH of 2.7, the OD_{600} increased from zero to 0.8 on day 2, while at lower initial pH of 2.3 and 2.5 it remained zero. From day 2 onwards, the

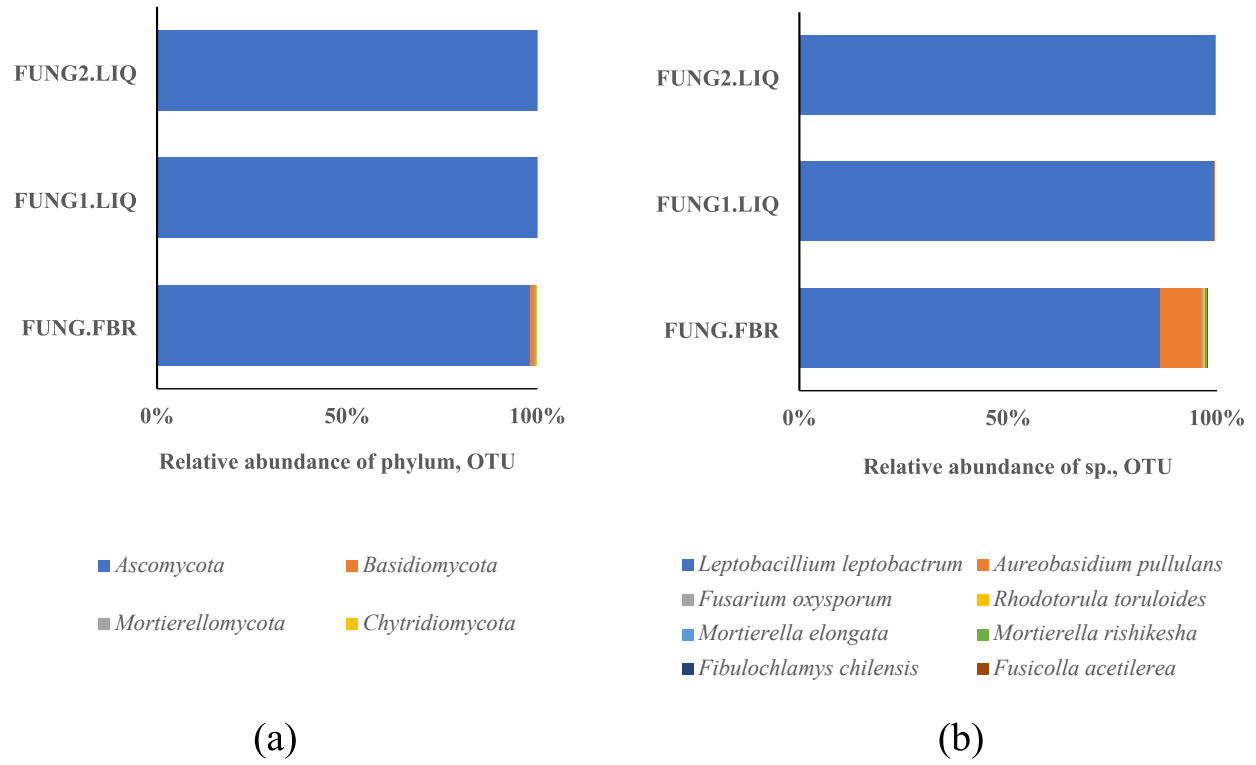

Fig. 3. Relative abundance of the composition of the microbial community in the FBR carrier material (FUNG.FBR) and samples of the isolated fungus (FUNG1.LIQ and FUNG2.LIQ). The OTUs were obtained by clustering with 97% identity on the effective tags of all samples.

OD_{600} with initial pH of 2.3 and 2.5 started to increase, however, the increase was slower than with initial pH of 2.7 (Fig. S2a). During incubations, the pH either remained constant or slightly decreased (Fig. S2b). These results show that decreasing the initial pH led to a decrease in OD_{600} and that initial pH of $\leq$2.5 considerably controlled the growth of *L. leptobactrum*.

The gluconate concentration effect was evaluated in a YE medium with 10 g/l glucose or without glucose. The growth of *L. leptobactrum* as measured by OD_{600} were higher in the glucose-containing media than those obtained in the glucose-free media (Fig. 4a, b). The pH either remained constant or slightly increased during incubation. The pH increase in the glucose-free media was more than in the glucose-containing media (Fig. S3a, b). The gluconate concentration in both the glucose-containing and glucose-free media remained constant (Fig. S4a, b), indicating that gluconate was not utilized by *L. leptobactrum*. No gluconic acid production by *L. leptobactrum* occurred during any of the experiments (data not shown). Glucose utilization by *L. leptobactrum* considerably decreased with increasing potassium gluconate concentration. With 125 and 150 g/l potassium gluconate, about 70% of the supplied glucose remained un-utilized (Fig. 4c). *G. oxydans* oxidized glucose at significantly higher rate than *L. leptobactrum* at high potassium gluconate concentrations. *G. oxydans* oxidized glucose within 2 days at all tested gluconate concentrations (Fig. 4d). The results show that increasing the concentration of gluconate in *L. leptobactrum* media resulted in a decrease in OD_{600} and glucose consumption rate. The results also show that *L. leptobactrum* did not utilize gluconate as carbon or energy source.

In summary, the results show that both low pH and high gluconate concentration control the growth of *L. leptobactrum*. Thus, maintaining the pH at $\leq$2.5 and/or the gluconate concentration at $\geq$100 g/l during FBR operation potentially provides a selective preference for *G. oxydans* over *L. leptobactrum*.

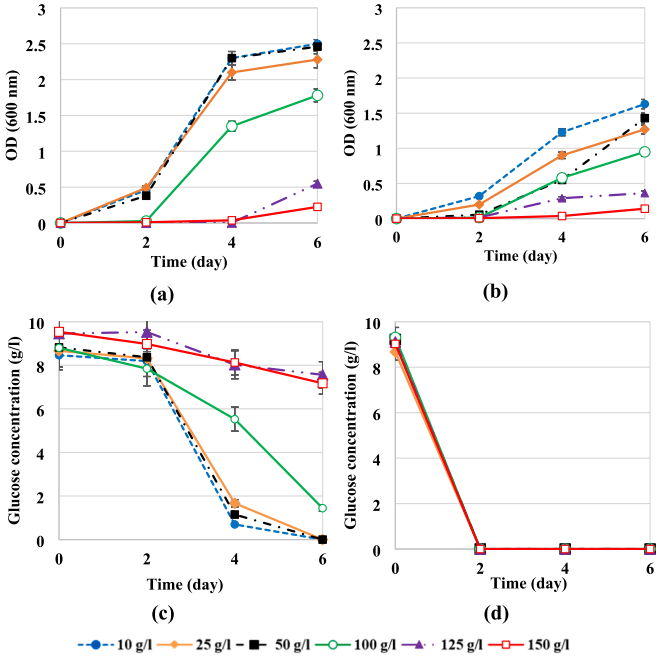

Fig. 4. Increase of optical density (OD_{600}) in *Leptobacillium leptobactrum* culture (a) with 10 g/l glucose, and (b) without glucose; and glucose utilization by (c) *Leptobacillium leptobactrum*, and (d) *Gluconobacter oxydans*; in presence of different potassium gluconate concentrations.

3.3. Continuous operation of *G. oxydans*-amended FBR

The aim of the FBR experimentations was to develop a bioprocess that favors glucose-to-gluconic acid bioconversion by *G. oxydans* and simultaneously controls interfering fungal contamination. Based on the

previous bioassay results, the operational strategy involved maintaining high gluconate concentration and/or low pH within the FBR.

During the start-up phase (day 0 to 5) of continuous FBR operation, 100 g/l potassium gluconate was supplemented to the YE medium in both the start solution and the feed. The changes in feed composition and flow rate during the start-up phase were shown in Fig. 1. By removing potassium gluconate from the feed on day 3 and increasing the feed flow rate from 0.15 ml/min (HRT 10.1 h) to 0.24 ml/min (HRT 6.3 h) on day 4, the effluent pH started to decrease, indicating the onset of glucose-to-gluconic acid bioconversion by *G. oxydans*. The effluent gluconate concentration gradually decreased to ~48 g/l on day 5 (Fig. 5). To avoid further decrease in gluconate concentration and to support FBR pH decrease to ≤2.5 by gluconic acid production, the feed glucose was increased to 50 g/l. After this change, the effluent's pH decreased to 2.4 by day 10 and remained constant thereafter.

During the continuous operation from day 5 to day 46, glucose loading rate was increased stepwise from 190 to 285 and 380 g/l•d (Fig. 6a), while the HRT was maintained constant at 6.3 h. The feed pH was unadjusted except for the period of day 29 to 46 with the glucose loading rate of 380 g/l•d (Fig. 6b), where the stepwise increase of feed pH was done to further enhance glucose-to-gluconic acid bioconversion.

During the FBR operation with glucose loading rate of 190 g/l•d, initial gluconic acid production rate was ~185 g/l•d (mean from day 5–8) and then it slightly decreased to ~160 g/l•d (mean from day 10–12). Simultaneously with the decrease of gluconic acid production rate, 5-ketogluconic acid production rate increased to about 18 g/l•d (Fig. 6c). During this period, the concentration of unutilized glucose in the effluent was between 1 and 3 g/l (Fig. 6d) and the average glucose-to-gluconic acid production yields were 89% and 77%, respectively (Fig. 5e).

With further increase of glucose loading rate from 190 to 285 g/l•d (day 13–20), the gluconic acid production rate increased to ~253 g/l•d and the glucose-to-gluconic acid conversion yield increased to ~81%. During this period, the 5-ketogluconic acid production rate was ~8 g/l.d and the unutilized glucose remained at ~10 g/l.

With further increase of the glucose loading rate to 380 g/l•d (day 21–29), the gluconic acid production rate and the glucose-to-gluconic acid conversion yield increased to ~360 g/l•d and 87%, respectively.

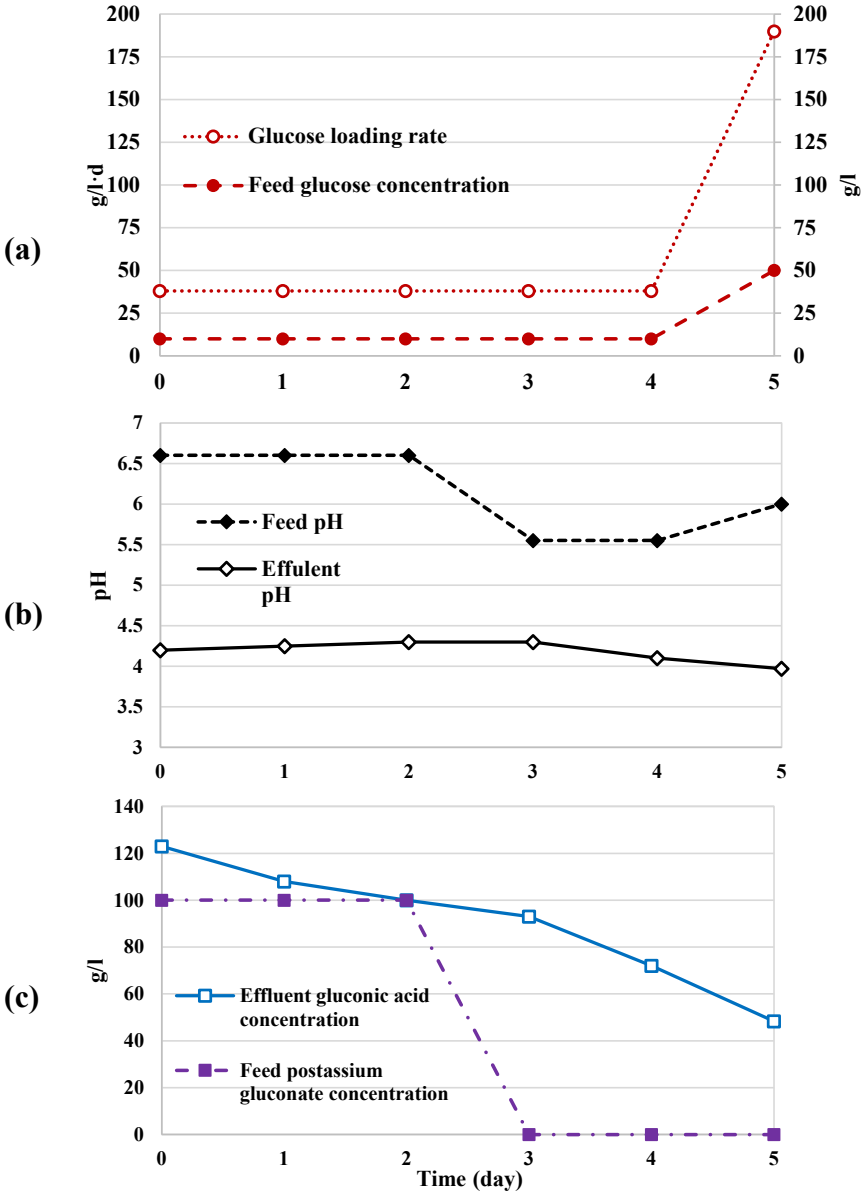

Fig. 5. Performance of *G. oxydans*-amended FBR during start-up.

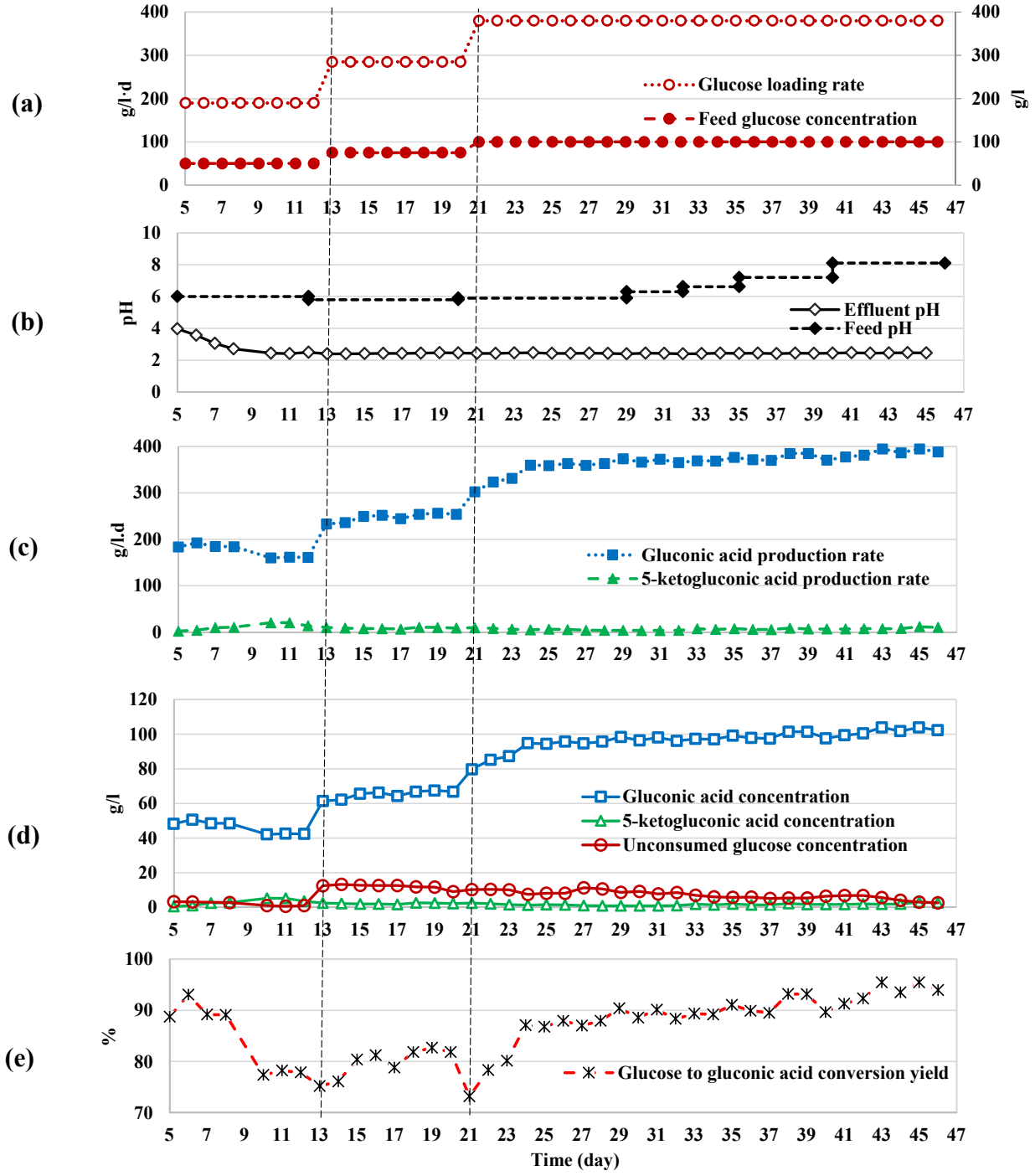

Fig. 6. Performance of *G. oxydans*-amended FBR during continuous operation. The vertical dotted lines separate the periods with different glucose loading rates.

During this period, the 5-ketogluconic acid production rate was ~4 g/l•d and the unused glucose concentration was ~9 g/l.

To further increase the glucose-to-gluconic acid bioconversion at the constant glucose loading rate of 380 g/l•d, the feed pH was stepwise increased to compensate for the pH decrease by gluconic acid production. With the increase of the feed pH from 5.9 on day 29 to 8.1 on day 41, the gluconic acid production rate increased from ~360 g/l•d to 390 g/l•d together with the decrease of remaining glucose concentration from ~9 g/l to ~3 g/l, respectively. At this condition, the glucose-to-gluconic acid conversion yield increased from 87% to 94%. The 5-ketogluconic acid production rate also increased from ~4 g/l•d to ~8 g/l•d. At all loading rates, DO remained 0.05 mg/l or below in the FBR system.

After 46 days of continuous operation of the FBR, *G. oxydans* biomass was estimated by DAPI cell counting using light microscopy. Total bacterial DAPI counts were made for samples from both the FBR AC carrier material and the liquid medium. The total bacterial count for the AC was higher than that of the liquid medium (Table 2). Based on the results, approximately 73% of the cells were on the AC and 27% remained in the liquid phase. In addition, the DAPI stained microscopic images (Fig. S5) indicated that *G. oxydans* was the dominant species inside the FBR, suppressing activity of contaminant cells.

These results demonstrate that high-rate and -yield glucose-to-gluconic acid bioconversion was obtained in *G. oxydans*-amended FBR by maintaining the operational conditions such that they favored

Table 2
Total bacterial counts of DAPI stained cells from samples of the FBR activated carbon carrier (wet and dry mass) and the liquid medium. 1 g of wet activated carbon equals 0.58 g dry activated carbon. w.w.: wet weight; d.w.: dry weight; w.v.: wet volume.

	Activated carbon	Liquid medium
cells/g w.w.	$8.07 \pm 0.55 \bullet 10^{9}$	–
cells/ g d.w.	$1.39 \pm 0.1 \bullet 10^{10}$	–
cells/ml	–	$1.13 \pm 0.2 \bullet 10^{9}$
cells/ml w.v	$9.45 \pm 0.55 \bullet 10^{10}$	–
cells/total w.w. or w.v (99.65 g = 85 ml)	$8.04 \pm 0.55 \bullet 10^{11}$	–
cells/ total volume of liquid medium (263.5 ml)	–	$2.97 \pm 0.2 \bullet 10^{11}$

G. oxydans and simultaneously discouraged contaminant activity in the not-fully aseptic system.

3.4. Bioleaching of spent NiMH battery with the FBR effluent

Bioleaching of REEs and base metals from the spent NiMH battery powder was investigated using effluent solutions produced by *G. oxydans*-amended FBR under different glucose loading rates of 190, 285, and 380 g/l•d (equivalent feed glucose concentrations 50, 75, 100 g/l). The aim was to evaluate the leaching efficiency of the metals at different spent battery powder pulp densities and effluent qualities.

One day leaching of 1% (w/v) spent NiMH battery with the gluconic acid solution obtained with 190 g/l•d glucose loading rate led to %-solubilization of 35 Zn, 55 Mn, 70 Fe, 56 Co, 29 Ni, and 37 total REEs. On day 7, the percent leaching yields increased to 80 Zn, 85 Mn, 80 Fe, 82 Co, 61 Ni, and 53 total REEs (Fig. S6). The obtained leaching yields for the major base metals and REEs of Mn, Co, Ni, La, Ce and Nd corresponded to metal concentrations as high as 187, 744, 2666, 590, 345, and 129 mg/l, respectively (Fig. 7).

The average total %-leaching yields obtained with glucose loading rates of 190, 285, and 380 g/l•d, were respectively, 78, 81, and 82 for the base metals and 53, 55, and 54 for the REEs (1% w/v pulp density, 7 days leaching). This indicated that the increase in gluconic acid production in result of increasing glucose loading rate in the FBR, did not significantly improve REEs or base metals leaching yields (Figs. S6, S7, S8). By increasing the spent battery pulp density from 1% to 10% (w/v), the average total %-leaching yields with glucose loading rates of 190, 285, and 380 g/l•d, decreased to 24, 28, and 38 for the base metals and to 14, 16, and 19 for the REEs. This indicated that increasing the spent battery pulp density considerably decreased both REEs and base metals solubilization with all FBR effluents.

In summary, the results show that high base metals and REEs leaching yields of 78–82% and 53–55% were achievable with the FBR effluents. The leaching yields decreased with the decrease of leaching duration or increase of the spent battery pulp density. Furthermore, higher gluconic acid production in result of increasing the FBR glucose loading rate to above 190 g/l•d did not lead to increased REE or base metal bioleaching yields.

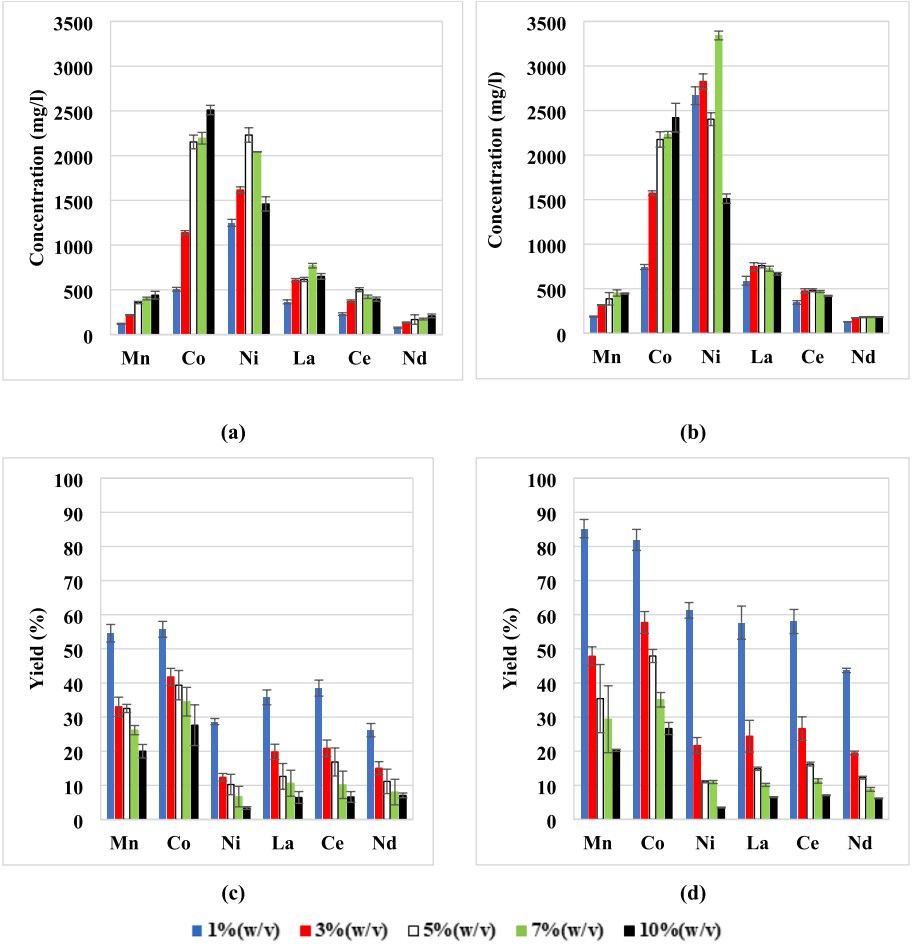

Fig. 7. Major base metals and REEs leaching concentrations and yields obtained with the FBR effluent from 190 g/l•d glucose loading rate (50 g/l feed glucose) containing 42 g/l gluconic acid and ~ 5 g/l 5-ketogluconic acid after (a, c) 1 day and (b, d) 7 days of leaching.

4. Discussion

This study developed and verified operation strategy for high-rate and -yield glucose-to-gluconic acid bioconversion in *G. oxydans*-amended FBR for efficient solubilization of REEs and base metals from spent NiMH battery powder.

4.1. Ecological engineering strategy for FBR operation

One of the main challenges of bioprocess scale-up for production of desired metabolite, is the asepticity requirements due to the high contamination risks [29]. This is of great concern especially while using glucose as carbon and energy source under aerobic and close to neutral conditions [7,30]. Glucose is a very common substrate for a huge range of aerobic microorganisms (Tables 3 and 4). For this reason, a specific operation strategy was required for the *G. oxydans*-amended FBR to maintain efficient glucose-to-gluconic acid bioconversion where full aseptic conditions could not be provided. The developed FBR operation strategy consisted of the following steps:

First, a fully mixed bioreactor system was selected. FBR provides fully mixed conditions due to high recycle rate as compared to the feed flow rate [31]. In a fully mixed bioreactor, the environmental conditions for the carrier bound microorganisms are very close to those of the effluent quality. Moreover, retaining active cells onto or within the carrier material as biofilm in the FBR provides long cell retention time compared to the hydraulic retention time and thus, allows to achieve high productivities [32].

Second, the growth conditions providing a selective advantage over potential competitive microorganisms were defined. In the *G. oxydans*-amended FBR, airborne fungal contamination was almost imminent in the first two trials (Fig. 3 and S1). Therefore, in a series of batch assays, the selectively advantageous conditions for *G. oxydans* over the fungal contaminant, *L. leptobactrum* were defined. These included high gluconate concentration of preferably ≥100 g/l and low pH of ≤2.5 under which conditions *L. leptobactrum* growth was significantly retarded. *G. oxydans* tolerates such high gluconate concentrations and low pH values under continuous operation conditions [18,33]. Moreover, the very high glucose oxidation rate of *G. oxydans* (Fig. 4c, d) leaves little glucose or DO available for *L. leptobactrum*, further retarding the contaminant growth.

Third, the FBR operation was started and maintained at high gluconate concentration and low pH and DO conditions. To achieve this in the start-up phase, glucose feed was supplemented with potassium gluconate. Once continuous glucose-to-gluconic acid conversion started, high gluconic acid concentration and low pH were provided by *G. oxydans* and thus, only glucose was fed. High oxygen consumption rates resulted in low DO in the FBR which also controlled contaminant activity. For large scale applications, the required gluconate for start-up phase could be provided via batch pre-cultivation of *G. oxydans* instead of using chemically available potassium gluconate.

Fourth, to obtain the highest possible gluconic acid production yields, the feed pH was increased stepwise while maintaining the glucose loading at highest rate of 380 g/l•d. Increasing the feed pH allowed more gluconic acid to be produced prior to pH becoming growth limiting in the FBR. The high gluconic acid concentration together with the constant acidic pH in the FBR (~2.4) and the low DO (≤0.05 mg/l) during the continuous operation provided an ecologically engineered and a highly contaminant resistant system for high-rate and -yield glucose-to-gluconic acid bioconversion with *G. oxydans*. The high-rate glucose to gluconic acid oxidization by *G. oxydans* results in high rate oxygen consumption [30,34] and, therefore, low DO within the FBR. This is another selective factor against fungal growth that also controls further oxidation of gluconic acid to ketogluconic acids [35].

This ecological engineering strategy is analogous to continuous thiosulfate biotransformation by haloalkaliphilic *Thioalkalivibrio versutus*-amended FBR where possible contaminant activity was suppressed

Table 3
Comparison of gluconic acid production rate and yield of the present study with the existing literature.

Experimental conditions							Performance indicators		
Bioreactor type	Operational mode	Microorganism	Substrate (g/l)	In-reactor pH	Temp (°C)	HRT (h)	Gluconic acid production rate (g/l·d)	Glucose-to-gluconic acid conversion yield (%)	Reference
Internal-loop airlift reactor[1]	Batch	*Aspergillus niger*	Glucose (200)	5.5–6.5	30	_	84 – 96	93	[17]
stirred tank reactor[1]	Batch	*Aureobasidium pullulans*	Glucose (80)	5.0–6.5	28	_	67	99	[22]
Cascade of two chemostats[1]	Continuous	*Aureobasidium pullulans*	Glucose (450)	6.5	30	19.5–24	334 – 305	60.4 – 84.4	[16]
Cascade of two chemostats[1]	Continuous	*Aureobasidium pullulans*	Glucose (600)	6.5	30	22	398	70.3	[16]
Immobilized mycelia recirculation bioreactor (cellulose carrier)	Batch	*Aspergillus niger*	Glucose (150)	6.0	30	_	157	96	[32]
Stirred tank reactor[1]	Batch	*Aspergillus niger*	Glucose (150)	5.5–6.5	30	_	110	92	[23]
Stirred fermentor[1]	Continuous	*Gluconobacter oxydans*	Sugarcane juice glucose (61.4)	4.35	30	6.6	161	94	[20]
Stirred fermentor[1]	Batch	*Gluconobacter oxydans*	Corn stover Glucose (125)	5.5	30	_	99	97	[21]
Stirred tank reactor[1]	Continuous	*Gluconobacter oxydans*	Glucose (40)	2.19	30	20	40		[24]
Stirred tank reactor[1]	Fed-batch	*Penicillium variabile*	Glucose (105)	5.0	28		48	99	[19]
Immobilized cell reactor (fibrous nylon carrier)	Continuous	*Gluconobacter oxydans*	Glucose (100)	2.5	30	NR	127	73	[18]
Fluidized bed reactor (activated carbon carrier)	Continuous	*Gluconobacter oxydans*	Glucose (100)	2.4	27	6.3	390	94	This study

1: aseptic system; NR = Not reported; Temp = Temperature.

Table 4
Heterotrophic REE bioleaching studies with different waste materials and microorganisms.

Waste material	Identified REEs	Experimental conditions					Bioleaching results		Ref
		Microorganism	Pulp density (% wt/v)	Leach time (day)	Sugar used (conc. as g/l)	Phosphate salt (conc. as g/l)	Total REE leaching yield (%)	%REE leached/g sugar used · day	
Blast furnace slag	La, Ce, Nd, Er	*Gluconobacter oxydans*	5	12	glucose (100)	-	51.55	0.04	[49]
FCC catalyst	Y, La, Ce, Pr, Nd, Sm, Eu, Gd, Tb, Ho, Dy, Er, Tm, Yb, Lu, Th	*Gluconobacter oxydans*	1.5	1	glucose(10)	KH_2PO_4 (0.37)	49	4.9	[15]
FCC catalyst	La	*Aspergillus niger*	5	3	glucose(60)	KH_2PO_4 (1) K_2HPO_4 (1)	74	0.4	[14]
FCC catalyst	La	*Aspergillus niger*	1	21	sucrose (100)	KH_2PO_4 (0.5)	63	0.03	[45]
Fluorescent phosphors	Y, La, Ce, Pr, Nd, Sm, Eu, Gd, Tb, Ho, Dy, Er, Tm, Yb, Lu, Th	*Gluconobacter oxydans*	1.5	1	glucose(10)	KH_2PO_4 (0.37)	2	0.2	[15]
Fluorescent phosphors	Y, La, Ce, Eu, Gd, Tb	Symbiotic mixed culture of Kombucha	2.85	14	glucose (100)	-	6.5	0.005	[12]
Fluorescent phosphors	Y, La, Ce, Eu, Gd, Tb	*Komagataeibacter Xylinus*	2.85	14	glucose (100)	-	12.6	0.009	[6]
Spent NiMH battery	Y, La, Ce, Pr, Nd, Sm, Gd, Er, Yb	*Gluconobacter Oxydans*	1	14	glucose(10)	K_2HPO_4 (0.47)	9	0.07	[50]
Spent NiMH battery	Y, La, Ce, Pr, Nd, Sm, Gd, Er, Yb	*Gluconobacter Oxydans*	1	1	glucose(10)	-	19.5	1.95	[13]
Spent NiMH battery	Y, La, Ce, Pr, Nd, Sm, Gd, Er, Yb	*Gluconobacter Oxydans*	1	1	glucose (50)	-	37	0.74	This study
Spent NiMH battery	Y, La, Ce, Pr, Nd, Sm, Gd, Er, Yb	*Gluconobacter Oxydans*	1	7	glucose (50)	-	53	0.15	This study

by high salinity (17.5 g Na^+/l) and alkaline pH of 10 [36]. This approach has been successfully applied also for high-rate iron oxidation in FBR systems with mixed cultures to produce concentrated ferric sulfate solutions [27]. In this system, high ferric iron concentration selected for *Leptospirillum ferriphilum* that tolerated higher Fe^{3+} concentrations than other iron oxidizers.

4.2. Maintaining high-rate and yield glucose-to-gluconic acid bioconversion

Suitable glucose concentration and feeding rate for a given microorganism depends on bioreactor configuration and the operation mode such as aeration [22]. In this study, with increase of the feed glucose concentration from 50 to 100 g/l, the gluconic acid production by *G. oxydans* in the FBR increased (Fig. 6). In high recirculation FBRs, the glucose concentrations for the carrier-bound microorganisms remain at close to effluent concentrations rather than the feed concentrations. Thus, high rate glucose oxidation by *G. oxydans* in this study FBR was rather controlled by dissolved oxygen limitation [22] than the feed glucose concentration. For comparison, in stirred tank reactors (STR), high glucose concentration was reported to increase gluconic acid production due to stimulation of expression of glucose oxidizing enzymes, as reported for microorganisms such as *Cryptococcus podzolicus* [37], *Aureobasidium pullulans* [22]. In the literature, a large range of feed glucose concentrations (40 – 600 g/l) have been reported for gluconic acid production by various microorganisms in different aseptic bioreactors (Table 3).

The gluconic acid production rates and yields of *G. oxydans*-amended FBR in this study were significantly higher than those reported for other microorganisms and bioreactors operated in batch, fed-batch or continuous mode (Table 3). Anastassiadis et al. [16] reported gluconic acid production rate of 398 g/l•d in an aseptically operated cascade of two chemostat bioreactors concluding that it was the highest rate reported in international literature in the last 100 years for the continuous production of gluconic acid or any microbial metabolite under continuous chemostat cultivation. In this work, albeit fully aseptic conditions could not be provided for the FBR, similar gluconic acid production rate (390 g/l•d) with significantly shorter HRT (6.3 h vs 22.0 h) and higher glucose-to-gluconic acid conversion yield (94% vs 70.3%) were obtained. The obtained gluconic acid production rates were controlled by the capacity of oxygen supply in the laboratory scale FBR system. In large scale systems, significantly more efficient oxygen supply is technically obtainable indicating potential for even higher gluconic acid production rates than reported here.

For efficient gluconic acid production by *G. oxydans*, pH needs to be maintained at $2 < pH < 5$ to inhibit further oxidation of gluconic acid to its keto-derivatives [38,39] together with avoiding pH becoming growth limiting [40]. During continuous operation of the *G. oxydans*-amended FBR of this study, glucose-to-gluconic acid conversion yields of 77%-87% were maintained at acidic pH of 2.4 without mechanical pH control. However, increasing the feed pH increased gluconic acid production while the FBR pH remained constant at 2.4. Stepwise increase of the feed pH from 5.9 to 8.1 with 100 g/l feed glucose concentration (380 g/l•d glucose loading rate) led to production of 390 g/l•d gluconic acid with a glucose-to-gluconic acid conversion yield of 94% at HRT of 6.3 h (Fig. 6).

Furthermore, the operational pH of our FBR was maintained at 2.4 without pH adjustment whereas in the cascade chemostat bioreactors it was maintained at 6.5 by continuous buffering. In addition to saving in buffering costs, the low pH operation of FBR controlled the system from fungal contamination. Also the high glucose-to-gluconic acid conversion yield and the short HRT of the non-asptically operated FBR addressed the requirements for a low-cost bioprocess. Low glucose-to-gluconic acid conversion yield process would leave glucose to the effluent resulting in high operational costs [24]. Long HRT i.e. slow production rate together with a full asepticity requirement results in large size bioreactor demands with high investment costs [16].

In summary, *G. oxydans*-amended FBR enabled very high-rate and -yield continuous production of gluconic acid. These proof of concept results are attractive not only for economic and industrial gluconic acid production but also for large-scale application of heterotrophic bioleaching in metal recovery/recycling. However, further studies such as scale-up are required prior to techno-economic evaluation of industrial applicability.

4.3. High-yield bioleaching

Non-contact bioleaching method was applied to solubilize REEs and base metals from spent NiMH batteries as contact bioleaching processes suffer from challenges such as (1) high contamination risks due to exposure of the microbial medium to non-aseptic metal-containing solid material, (2) retarded microbial growth rate due to toxicity of metal-containing material, and (3) slow leaching rates due to reduced microbial leaching agent production [7,41]. Non-contact bioleaching method allows for separate optimization of bioleaching agent production and metal leaching steps. Thus, neither the biological leaching agent production would be affected by the metal-containing solid material, nor optimization of the metal leaching from the solid material would be constrained by the microbial growth limits such as temperature and/or pH tolerance [7,42]. The mechanisms and reactions in REE bioleaching systems have been recently reviewed by Rasoulnia et al., [7].

Growing biofilm-embedded, immobilized microorganisms enables continuous production of microbial leaching agents in a separate bioreactor to do non-contact bioleaching [7]. In this study, a *G. oxydans*-amended FBR was developed for high-rate and -yield continuous production of gluconic acid to bioleach REEs and base metals from spent NiMH batteries. Using the FBR gluconic acid solution produced with 190 g/l•d glucose loading rate (50 g/l feed glucose concentration), high average total base metal and REE leaching yields of 78% and 53% were achieved for 1% w/v spent battery pulp density within 7 days. The obtained total REE leaching yield of 53% was higher than the yields obtained with similar high metal-grade sources of fluorescent phosphors (FP) and spent NiMH batteries, but quite close to those of lower metal-grade sources such as spent fluid catalytic cracking (FCC) catalysts and blast furnace slags (Table 4). The achieved REE leaching yield was notable as metal leaching from high metal-grade REE sources such as spent NiMH batteries is more difficult than from lower metal-grade REE sources. This is due to potential saturation effects in the solution and also because of presence of high amounts of base metals and other acid consuming materials which compete with REEs to react with the leaching agent [13]. However, in addition to the high metal content, REE bioleaching efficiency is also dependent on other factors such as the microorganism type, medium composition, type and amount of organic carbon source and the produced biolixiviant, REE bonding within the solid material and the leaching conditions [7].

By increasing the glucose loading rate to above 190 g/l•d, higher gluconic acid concentrations were produced in the FBR. Leaching with these effluents, however, did not further improve the REEs and base metals solubilization. This was because the metals in spent NiMH batteries exist in different forms of oxides, hydroxides, alloys, and pure metals, which have differing leaching capabilities [7,43]. It is likely that the gluconic acid production enhancement was not sufficient to solubilize the remaining metallic and alloy fractions of the spent NiMH batteries which are usually more resistant to leaching than the oxides and hydroxides [7].

Medium composition in this study played an important role. The utilized YE medium had an optimized YE/G ratio which allowed for high-yield conversion of glucose to gluconic acid. Moreover, the medium contained no phosphate salts such as K_2HPO_4 and KH_2PO_4 and thus minimized possibility of base metals and especially REEs precipitation with surpluses of dissolved phosphate in the medium during the leaching [13]. These phosphate salts act both as phosphorous source and buffering agent in microbial cultures and therefore have been commonly used in various heterotrophic REE bioleaching studies [14,15,44–48].

In summary, high-rate and -yield continuous production of gluconic acid in *G. oxydans*-amended FBR using a dissolved phosphorous deficient medium that minimized risk of metal precipitation during leaching, was an effective approach for non-contact bioleaching of REEs and base metals from spent NiMH batteries. This bioreactor system used for biolixiviant production has also potential for other metal-containing solid materials as the bioleaching agent production and the metal leaching steps are separately optimized.

5. Conclusions

This study validated an ecological engineering strategy for high-rate and -yield gluconic acid production in non-aseptic, *G. oxydans*-amended FBR for REEs and base metals leaching from spent NiMH batteries, allowing the following conclusions to be drawn:

- Glucose as close-to universal substrate for aerobic biodegradation represents a challenge for production of desired biotransformation products such as gluconic acid in an open bioreactor system. Without precautions, the FBR system becomes contaminated and massively overgrown by airborne fungi such as *L. leptobactrum*.
- Ecological engineering strategy for the high-rate glucose-to-gluconic acid bioconversion includes maintaining high gluconate concentration (50–100 g/l) and low pH (~2.4) together with high glucose utilization rate and the resulting very low DO within the non-aseptic and fully mixed *G. oxydans*-amended FBR system.
- During onset of FBR operation, supplementation of the glucose feed with gluconate together with pH decrease are required whereas during the operation desired conditions are provided by *G. oxydans* activity.
- By stepwise increase of the feed pH, high glucose-to-gluconic acid bioconversion rate and yield of up-to 390 g/l•d and 94% are attainable using the *G. oxydans*-amended FBR.
- With the FBR effluent, total REEs and base metals leaching yields of 53–55% and 78–82%, respectively, are attainable from 1% (w/v) spent battery within 7 days.

In summary, the non-aseptically operated *G. oxydans*-amended FBR was highly contaminant activity resistant and converted glucose to gluconic acid at one of the highest rates so far reported for any glucose biotransformation process. Further, the FBR effluent produced from concentrated glucose and dissolved phosphorous deficient feed minimized metal precipitation during leaching resulting in higher REE leaching yields from spent NiMH batteries than the earlier reports for such materials.

Declaration of Competing Interest

The authors declare that they have no known competing financial interests or personal relationships that could have appeared to influence the work reported in this paper.

Data availability

No data was used for the research described in the article.

Acknowledgements

The authors acknowledge AkkuSer Oy for providing the spent NiMH battery powder sample. The advice of Dr. Aino-Maija Lakaniemi and Mr. Robert Barthen during the planning and bioreactor startup phases is greatly appreciated. We also thank Dr. Johanna Rinta-Kanto for helping with the selection of DNA sequencing. Payam Rasoulnia acknowledges Tampere University Doctoral School for funding this research.

Appendix A. Supplementary data

Supplementary data to this article can be found online at https://doi.org/10.1016/j.cej.2023.142088.

References

[1] J.C.Y. Jung, P.C. Sui, J. Zhang, A review of recycling spent lithium-ion battery cathode materials using hydrometallurgical treatments, J. Storage Mater. 35 (2021), 102217, https://doi.org/10.1016/j.est.2020.102217.

[2] F. Liu, C. Peng, A. Porvali, Z. Wang, B.P. Wilson, M. Lundström, Synergistic recovery of valuable metals from spent nickel-metal hydride batteries and lithium-ion batteries, ACS Sustain. Chem. Eng. 7 (2019) 16103–16111, https://doi.org/10.1021/acssuschemeng.9b02863.

[3] M. Zhou, B. Li, J. Li, Z. Xu, Pyrometallurgical technology in the recycling of a spent lithium ion battery: evolution and the challenge, ACS ES&T Eng. 1 (2021) 1369–1382, https://doi.org/10.1021/acsestengg.1c00067.

[4] L. Omodara, S. Pitkäaho, E.M. Turpeinen, P. Saavalainen, K. Oravisjärvi, R. L. Keiski, Recycling and substitution of light rare earth elements, cerium, lanthanum, neodymium, and praseodymium from end-of-life applications – a review, J. Clean. Prod. 236 (2019), https://doi.org/10.1016/j.jclepro.2019.07.048.

[5] V. Innocenzi, N.M. Ippolito, I. De Michelis, M. Prisciandaro, F. Medici, F. Vegliò, A review of the processes and lab-scale techniques for the treatment of spent rechargeable NiMH batteries, J. Power Sources 362 (2017) 202–218, https://doi.org/10.1016/j.jpowsour.2017.07.034.

[6] S. Hopfe, S. Konsulke, R. Barthen, F. Lehmann, S. Kutschke, K. Pollmann, Screening and selection of technologically applicable microorganisms for recovery of rare earth elements from fluorescent powder, Waste Manag. 79 (2018) 554–563, https://doi.org/10.1016/j.wasman.2018.08.030.

[7] P. Rasoulnia, R. Barthen, A. Lakaniemi, A critical review of bioleaching of rare earth elements : The mechanisms and effect of process parameters, Crit. Rev. Environ. Sci. Technol. (2020) 1–50, https://doi.org/10.1080/10643389.2020.1727718.

[8] Y. Qu, B. Lian, Bioleaching of rare earth and radioactive elements from red mud using *Penicillium tricolor* RM-10, Bioresour. Technol. 136 (2013) 16–23, https://doi.org/10.1016/j.biortech.2013.03.070.

[9] L. Zhang, H. Dong, Y. Liu, L. Bian, X. Wang, Z. Zhou, Y. Huang, Bioleaching of rare earth elements from bastnaesite-bearing rock by actinobacteria, Chem. Geol. 483 (2018) 544–557, https://doi.org/10.1016/j.chemgeo.2018.03.023.

[10] D.E. Lazo, L.G. Dyer, R.D. Alorro, R. Browner, Treatment of monazite by organic acids I: Solution conversion of rare earths, Hydrometall. 174 (2017) 202–209, https://doi.org/10.1016/j.hydromet.2017.10.003.

[11] V.L. Brisson, W.-Q. Zhuang, L. Alvarez-Cohen, Bioleaching of rare earth elements from monazite sand, Biotechnol. Bioeng. 113 (2016) 339–348, https://doi.org/10.1002/bit.25823.

[12] S. Hopfe, K. Flemming, F. Lehmann, R. Möckel, S. Kutschke, K. Pollmann, Leaching of rare earth elements from fluorescent powder using the tea fungus Kombucha, Waste Manag. 62 (2017) 211–221, https://doi.org/10.1016/j.wasman.2017.02.005.

[13] P. Rasoulnia, R. Barthen, A.M. Lakaniemi, H. Ali-Löytty, J.A. Puhakka, Low residual dissolved phosphate in spent medium bioleaching enables rapid and enhanced solubilization of rare earth elements from end-of-life NiMH batteries, Miner. Eng. 176 (2022), https://doi.org/10.1016/j.mineng.2021.107361.

[14] M.P. Dewi, H.T.B.M. Petrus, N. Okibe, Recovering secondary REE value from spent oil refinery catalysts using biogenic organic acids, Catalysts 10 (2020) 1–15, https://doi.org/10.3390/catal10091090.

[15] D.W. Reed, Y. Fujita, D.L. Daubaras, Y. Jiao, V.S. Thompson, Bioleaching of rare earth elements from waste phosphors and cracking catalysts, Hydrometall. 166 (2016) 34–40, https://doi.org/10.1016/j.hydromet.2016.08.006.

[16] S. Anastassiadis, H.J. Rehm, Continuous gluconic acid production by the yeast-like *Aureobasidium pullulans* in a cascading operation of two bioreactors, Appl. Microbiol. Biotechnol. 73 (2006) 541–548, https://doi.org/10.1007/s00253-006-0499-y.

[17] J. Klein, M. Rosenberg, J. Markoš, O. Dolgoš, M. Krošlák, L. Krištofíková, Biotransformation of glucose to gluconic acid by *Aspergillus niger* – study of mass transfer in an airlift bioreactor, Biochem. Eng. J. 10 (2002) 197–205, https://doi.org/10.1016/S1369-703X(01)00181-4.

[18] P. Seiskari, Y.Y. Linko, P. Linko, Continuous production of gluconic acid by immobilized *Gluconobacter oxydans* cell bioreactor, Appl. Microbiol. Biotechnol. 21 (1985) 356–360, https://doi.org/10.1007/BF00249979.

[19] S. Crognale, M. Petruccioli, M. Fenice, F. Federici, Fed-batch gluconic acid production from *Penicillium variabile* P16 under different feeding strategies, Enzyme Microb. Technol. 42 (2008) 445–449, https://doi.org/10.1016/j.enzmictec.2008.01.002.

[20] S. Banerjee, R. Kumar, P. Pal, Fermentative production of gluconic acid: a membrane-integrated Green process, J. Taiwan Inst. Chem. Eng. 84 (2018) 76–84, https://doi.org/10.1016/j.jtice.2018.01.030.

[21] H. Zhang, G. Liu, J. Zhang, J. Bao, Fermentative production of high titer gluconic and xylonic acids from corn stover feedstock by *Gluconobacter oxydans* and techno-economic analysis, Bioresour. Technol. 219 (2016) 123–131, https://doi.org/10.1016/j.biortech.2016.07.068.

[22] S. Fernandes, I. Belo, M. Lopes, Highly aerated cultures boost gluconic acid production by the yeast-like fungus *Aureobasidium pullulans*, Biochem. Eng. J. 175 (2021), 108133, https://doi.org/10.1016/j.bej.2021.108133.

[23] H. Znad, J. Markoš, V. Baleš, Production of gluconic acid from glucose by *Aspergillus niger*: growth and non-growth conditions, Process Biochem. 39 (2004) 1341–1345, https://doi.org/10.1016/S0032-9592(03)00270-X.

[24] V.S. Thompson, M. Gupta, H. Jin, E. Vahidi, M. Yim, M.A. Jindra, V. Nguyen, Y. Fujita, J.W. Sutherland, Y. Jiao, D.W. Reed, Techno-economic and life cycle analysis for bioleaching rare-earth elements from waste materials, ACS Sustain. Chem. Eng. 6 (2018) 1602–1609, https://doi.org/10.1021/acssuschemeng.7b02771.

[25] R. Hajdu-Rahkama, B. Özkaya, A.M. Lakaniemi, J.A. Puhakka, Kinetics and modelling of thiosulphate biotransformations by haloalkaliphilic *Thioalkalivibrio versutus*, Chem. Eng. J. 401 (2020), 126047, https://doi.org/10.1016/j.cej.2020.126047.

[26] M. Gardes, T.D. Bruns, ITS primers with enhanced specificity for basidiomycetes - application to the identification of mycorrhizae and rusts, Mol. Ecol. 2 (1993) 113–118, https://doi.org/10.1111/j.1365-294X.1993.tb00005.x.

[27] P.H.M. Kinnunen, J.A. Puhakka, High-rate ferric sulfate generation by a *Leptospirillium ferriphilum*-dominated biofilm and the role of jarosite in biomass retainment in a fluidized-bed reactor, Biotechnol. Bioeng. 85 (2004) 697–705, https://doi.org/10.1002/bit.20005.

[28] A.-K. Halinen, N. Rahunen, A.H. Kaksonen, J.A. Puhakka, Heap bioleaching of a complex sulfide ore, Hydrometall. 98 (2009) 92–100, https://doi.org/10.1016/j.hydromet.2009.04.005.

[29] Z. Chen, C. Wan, Non-sterile fermentations for the economical biochemical conversion of renewable feedstocks, Biotechnol. Lett 39 (2017) 1765–1777, https://doi.org/10.1007/s10529-017-2429-8.

[30] W. Olijve, J.J. Kok, An analysis of the growth of *Gluconobacter oxydans* in chemostat cultures, Arch. Microbiol. 121 (3) (1979) 291–297.

[31] B. Özkaya, A.H. Kaksonen, E. Sahinkaya, J.A. Puhakka, Fluidized bed bioreactor for multiple environmental engineering solutions, Water Res. 150 (2019) 452–465, https://doi.org/10.1016/j.watres.2018.11.061.

[32] N.V. Sankpal, B.D. Kulkarni, Optimization of fermentation conditions for gluconic acid production using *Aspergillus niger* immobilized on cellulose microfibrils, Process Biochem. 37 (2002) 1343–1350, https://doi.org/10.1016/S0032-9592(01)00335-1.

[33] S. Wei, Q. Song, D. Wei, Repeated use of immobilized gluconobacter oxydans cells for conversion of glycerol to dihydroxyacetone, Prep. Biochem. Biotech. 37 (2007) 67–76, https://doi.org/10.1080/10826060601040954.

[34] J. Yuan, M. Wu, J. Lin, L. Yang, Enhancement of 5-keto-d-gluconate production by a recombinant *Gluconobacter oxydans* using a dissolved oxygen control strategy, J. Biosci. Bioeng. 122 (2016) 10–16, https://doi.org/10.1016/j.jbiosc.2015.12.006.

[35] M.A. Jindra, D.W. Reed, V.S. Thompson, D.L. Daubaras, Developing a scalable system for biorecovery of critical materials from industrial waste with *Gluconobacter Oxydans*, 2016. 10.2172/1504923.

[36] A. D'Aquino, R. Hajdu-Rahkama, J.A. Puhakka, Elemental sulphur production from thiosulphate under haloalkaline conditions in a *Thioalkalivibrio versutus* amended fluidized bed bioreactor, Biochem. Eng. J. 172 (2021), 108062, https://doi.org/10.1016/j.bej.2021.108062.

[37] X. Qian, O. Gorte, L. Chen, W. Zhang, W. Dong, J. Ma, M. Jiang, F. Xin, K. Ochsenreither, Co-production of single cell oil and gluconic acid using oleaginous *Cryptococcus podzolicus* DSM 27192, Biotechnol. Biofuels 12 (2019) 1–9, https://doi.org/10.1186/s13068-019-1469-9.

[38] G. Weenk, W. Olijve, W. Harder, Ketogluconate formation by *Gluconobacter* species, Appl. Microbiol. Biotechnol. 20 (6) (1984).

[39] M. Elfari, S.H. Christoph, M. Merfort, V. Khodaverdi, U. Herrmann, A *Gluconobacter oxydans* mutant converting glucose almost quantitatively to 5-keto- D -gluconic acid, (2005) 668–674. 10.1007/s00253-004-1721-4.

[40] A. Gupta, V.K. Singh, G.N. Qazi, A. Kumar, *Gluconobacter oxydans*: Its biotechnological applications, J. Mol. Microbiol. Biotechnol. 3 (2001) 445–456.

[41] Y. Yao, M. Zhu, Z. Zhao, B. Tong, Y. Fan, Z. Hua, Hydrometallurgical processes for recycling spent lithium-ion batteries: a critical review, ACS Sustain. Chem. Eng. 6 (2018) 13611–13627, https://doi.org/10.1021/acssuschemeng.8b03545.

[42] W.A.G. Hassanien, O.A.N. Desouky, S.S.E. Hussien, Bioleaching of some rare earth elements from egyptian monazite using *Aspergillus ficuum* and *Pseudomonas aeruginosa*, Walailak J. Sci. Technol. 11 (2014) 809–823, https://doi.org/10.2004/wjst.v11i6.481.

[43] M. Zielinski, L. Cassayre, P. Floquet, M. Macouin, P. Destrac, N. Coppey, C. Foulet, B. Biscans, A multi-analytical methodology for the characterization of industrial samples of spent Ni-MH battery powders, Waste Manag. 118 (2020) 677–687, https://doi.org/10.1016/j.wasman.2020.09.017.

[44] M.M. Amin, I.E. El-Aassy, M.G. El-Feky, A.M. Sallam, E.M. El-Sayed, A.A. Nada, N. M. Harpy, Fungal leaching of rare earth elements from lower carboniferous shales, southwestern Sinai, Egypt, Roman. J. Biophys. 24 (2014) 25–41.

[45] H.M. Mouna, S.S. Baral, A bio-hydrometallurgical approach towards leaching of lanthanum from the spent fluid catalytic cracking catalyst using *Aspergillus niger*, Hydrometall. 184 (2019) 175–182, https://doi.org/10.1016/j.hydromet.2019.01.007.

[46] M.J. Barnett, B. Palumbo-Roe, E.A. Deady, S.P. Gregory, Comparison of three approaches for bioleaching of rare earth elements from bauxite, Minerals. 10 (2020) 1–19, https://doi.org/10.3390/min10080649.

[47] S. Park, Y. Liang, Bioleaching of trace elements and rare earth elements from coal fly ash, Int. J. Coal Sci. Technol. 6 (2019) 74–83, https://doi.org/10.1007/s40789-019-0238-5.

[48] N. Reynier, R. Gagné-Turcotte, L. Coudert, S. Costis, R. Cameron, J.F. Blais, Bioleaching of uranium tailings as secondary sources for rare earth elements production, Minerals. 11 (2021) 1–21, https://doi.org/10.3390/min11030302.

[49] S. Abhilash, P. Hedrich, A. Meshram, A. Schippers, S.S. Gupta, Extraction of REEs from blast furnace slag by *Gluconobacter oxydans*, Minerals. 12 (2022) 1–9, https://doi.org/10.3390/min12060701.

[50] P. Rasoulnia, R. Barthen, K. Valtonen, A.M. Lakaniemi, Impacts of phosphorous source on organic acid production and heterotrophic bioleaching of rare earth

elements and base metals from spent nickel-metal-hydride batteries, Waste Biomass Valoriz. (2021), https://doi.org/10.1007/s12649-021-01398-x.